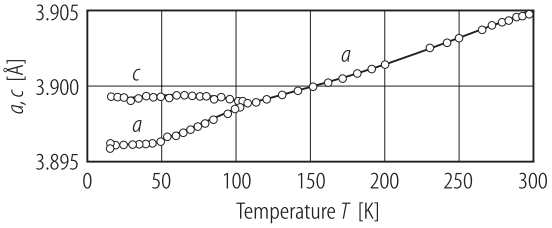

Fig. 1A-8-001. $SrTiO_3$. *a*, *c* vs. *T* [73Oka]. *a*, *c*: lattice constants (superlattice in phase II below 105 K is disregarded).

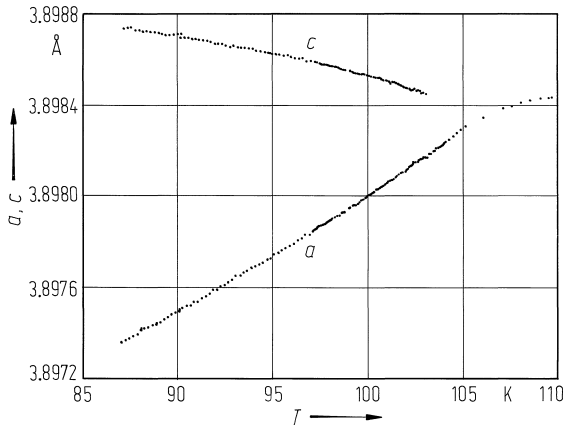

Fig. 1A-8-002. $SrTiO_3$. *a*, *c* vs. *T* [85Sat]. *a*, *c*: unit cell parameters.

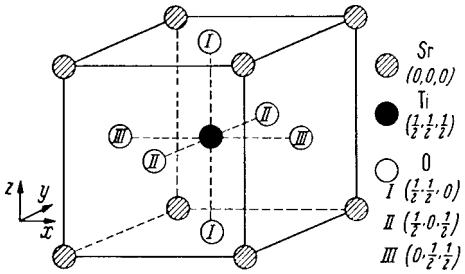

Fig. 1A-8-003. $SrTiO_3$. Crystal structure of phase I [64Cow].

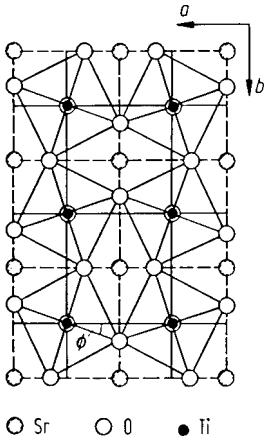

Fig. 1A-8-004. $SrTiO_3$. Schematic projection of the structure in low temperature phase II on (001) plane as determined by ESR experiment [67Uno].

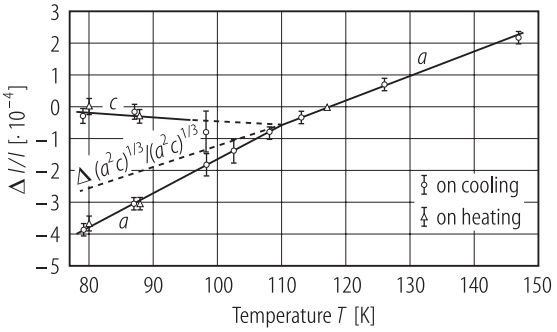

Fig. 1A-8-005. $SrTiO_3$. $\Delta l/l$ vs. T (along a and c) [69Ale].

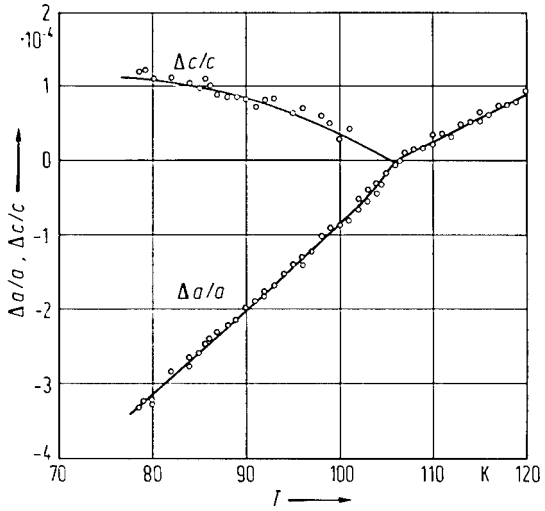

Fig. 1A-8-006. $SrTiO_3$. $\Delta a/a$, $\Delta c/c$ vs. T [74Oka].

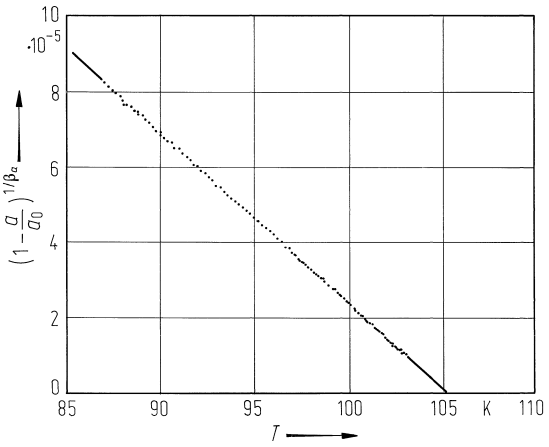

Fig. 1A-8-007. $SrTiO_3$. $(1 - a / a_0)^{1/\beta_a}$ vs. T [85Sat]. a: unit cell parameter, a_0: a at Θ_{II-I}. β_a = 0.88, a_0 = 3.898341 Å, Θ_{II-I} = 105.10 K.

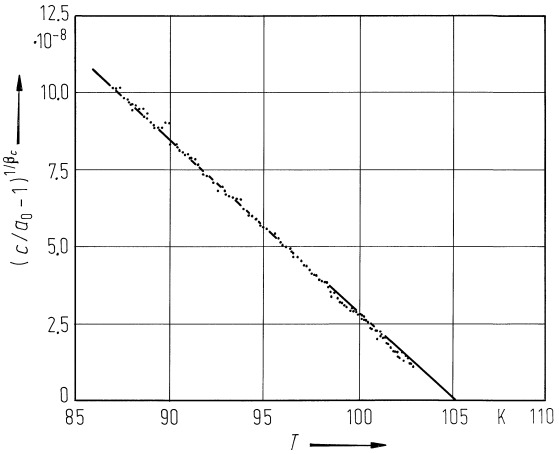

Fig. 1A-8-008. $SrTiO_3$. $(c/a_0 - 1)^{1/\beta_c}$ vs. T [85Sat]. c: unit cell parameter, a_0: see the caption of **Fig**. 1A-8-007. $\beta_c = 0.57$.

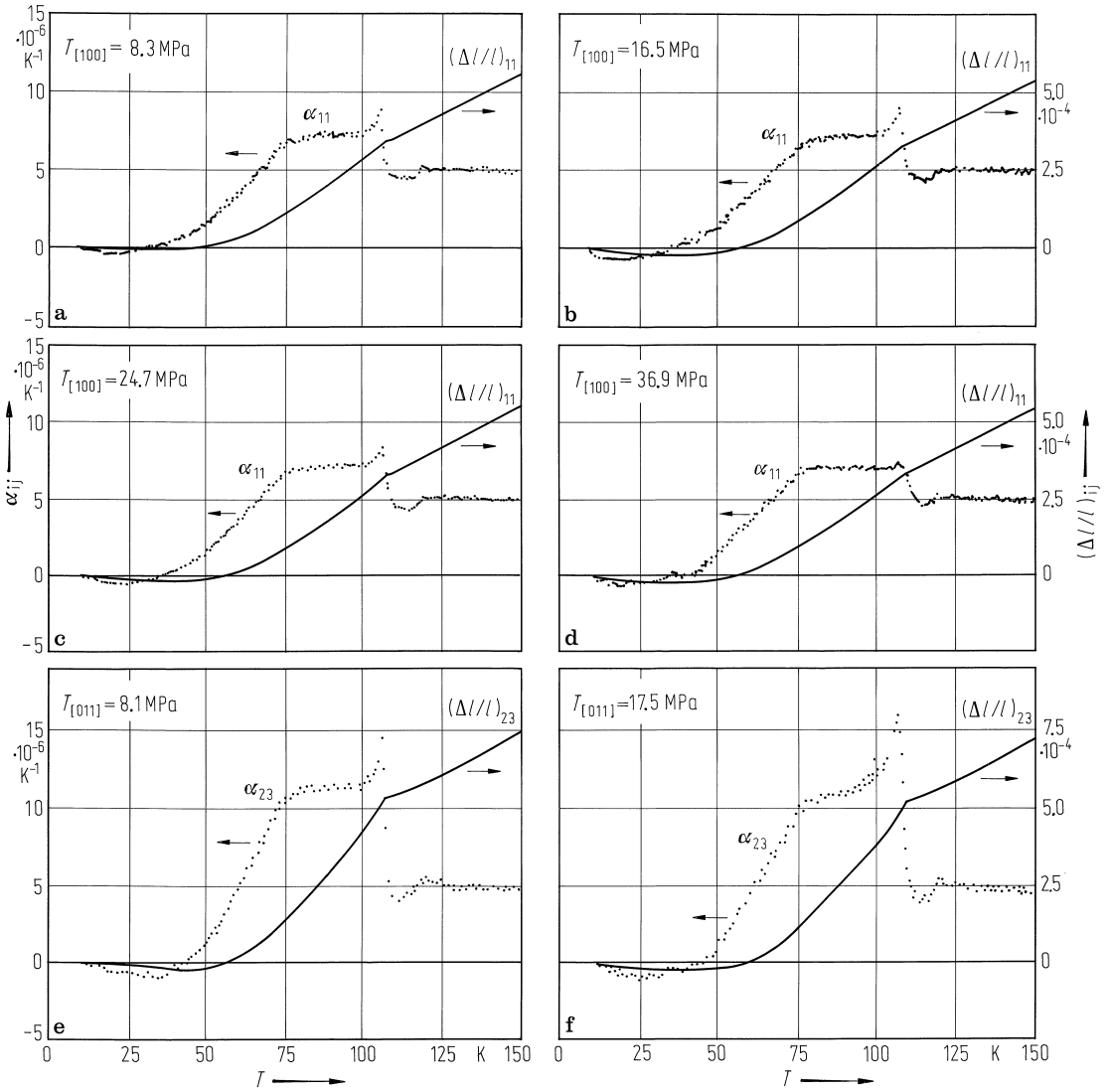

Fig. 1A-8-009. $SrTiO_3$. α_{ij}, $(\Delta l / l)_{ij}$ vs. T under compressive stress $\boldsymbol{T}$ [84Tsu]. α_{11}, α_{23} : linear thermal expansion coefficient along <100> and <011>, respectively. $(\Delta l / l)_{11}$, $(\Delta l / l)_{23}$: thermal dilatation. $\boldsymbol{T}_{[100]}$, $\boldsymbol{T}_{[011]}$: uniaxial compressive stress along <100> and <011>.

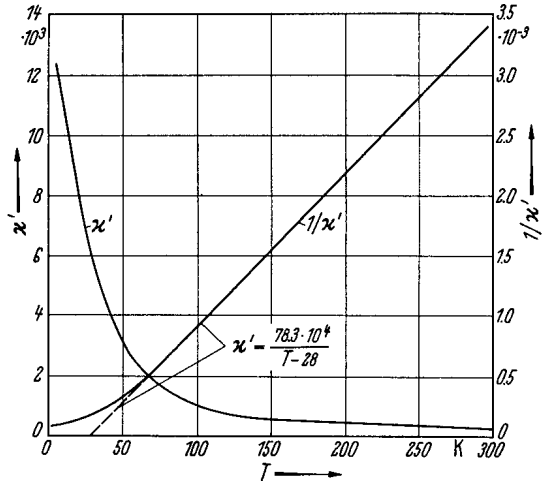

Fig. 1A-8-010. $SrTiO_3$. κ ', κ'^{-1} vs. T [61Mit]. *a*-cut crystal.

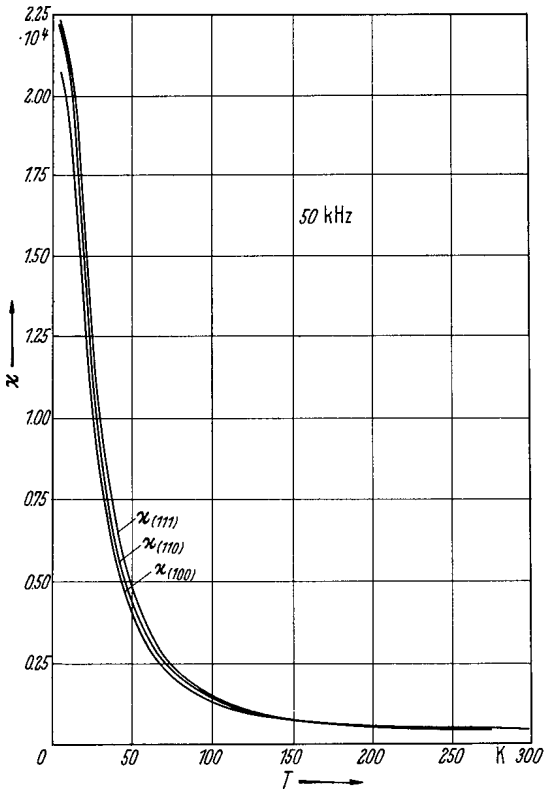

Fig. 1A-8-011. $SrTiO_3$. $\kappa_{(111)}$, $\kappa_{(110)}$, $\kappa_{(100)}$ vs. T [62Saw]. f = 50 kHz.

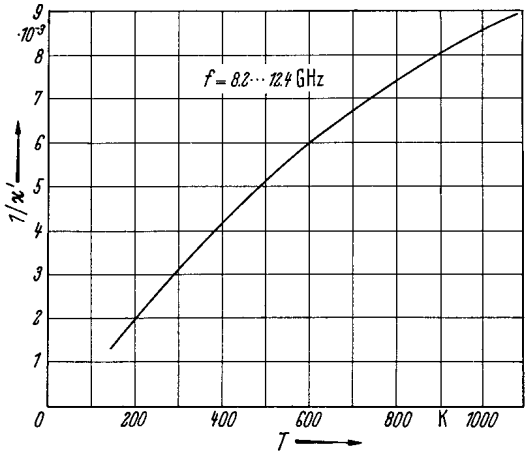

Fig. 1A-8-012. $SrTiO_3$. κ'^{-1} vs. T [64Rup].
f = 8.2...12.4 GHz (X-band).

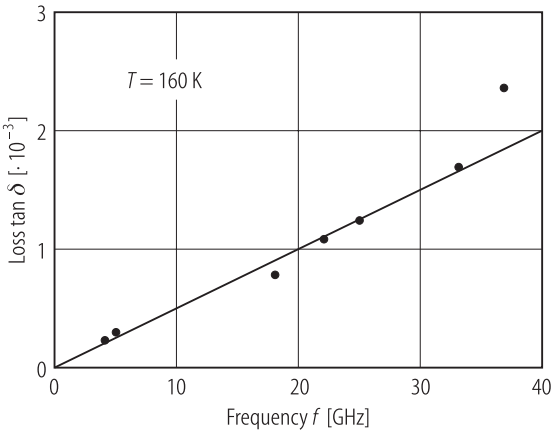

Fig. 1A-8-013. $SrTiO_3$. $\tan\delta$ vs. f [62Rup]. T = 160 K.

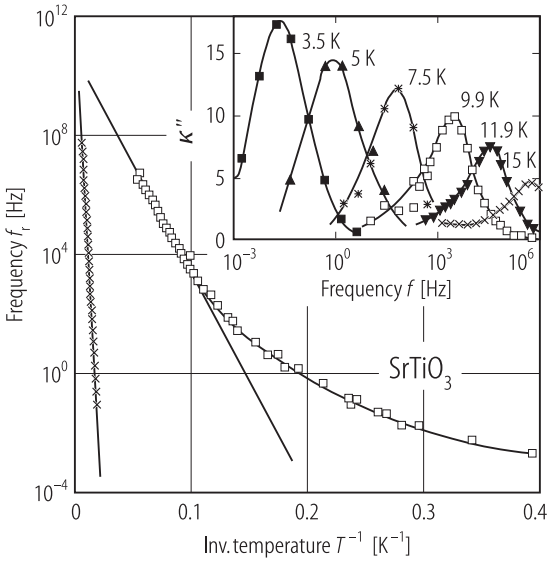

Fig. 1A-8-014. $SrTiO_3$. f_r vs. T^{-1} [94Via]. f_r: relaxation frequency. Insert shows κ'' vs. f for the low frequency dispersion.

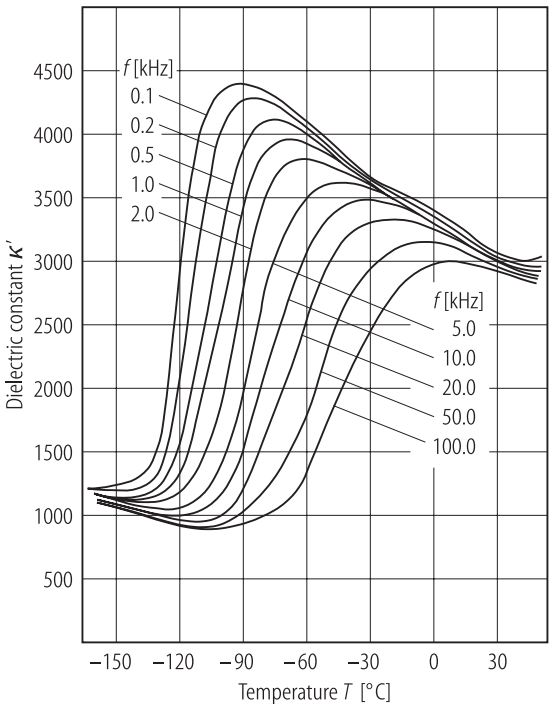

Fig. 1A-8-015. 0.96 $SrTiO_3$ · 0.04 $Er_{2/3}TiO_3$ (ceramics). κ' vs. T [70Joh]. Parameter: f.

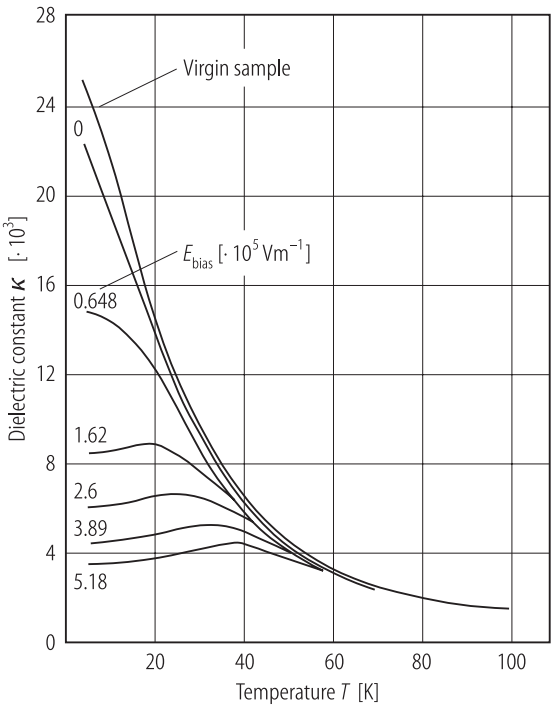

Fig. 1A-8-016. $SrTiO_3$. κ vs. T [70Sai]. Parameter: E_{bias}. Electric fields are along [100]. Specimen was not annealed. f = 1 kHz.

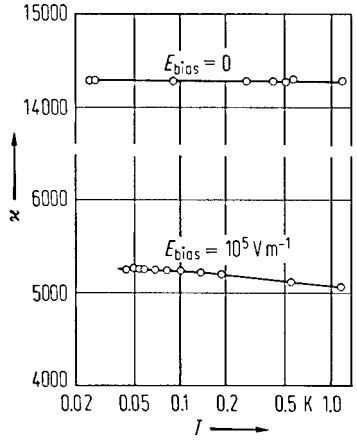

Fig. 1A-8-017. $SrTiO_3$. κ vs. T (at low temperatures) [73Fre]. Parameter: E_{bias}.

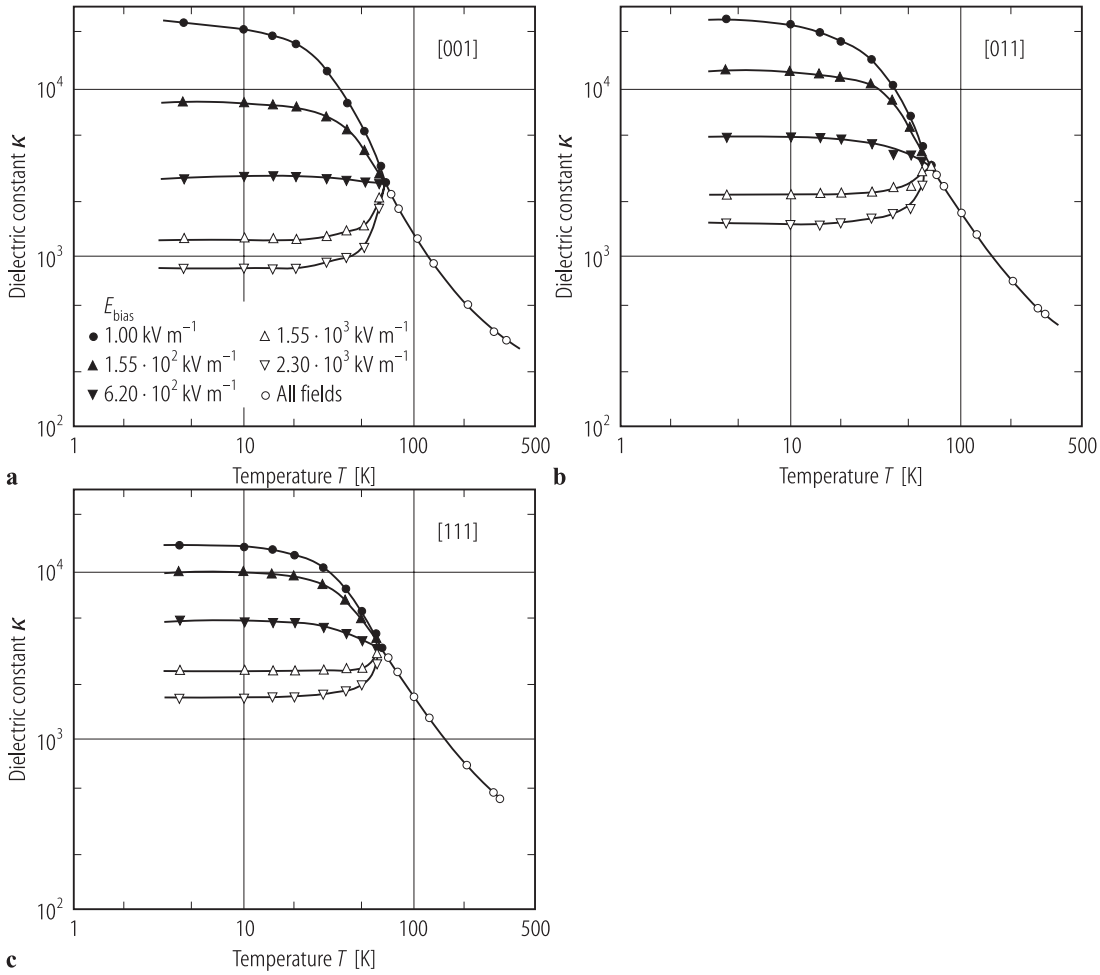

Fig. 1A-8-018. $SrTiO_3$. κ vs. T [72Nev]. Parameter: E_{bias}. Orientation: **(a)** [001], **(b)** [011], **(c)** [111]. f = 1 kHz...50 MHz.

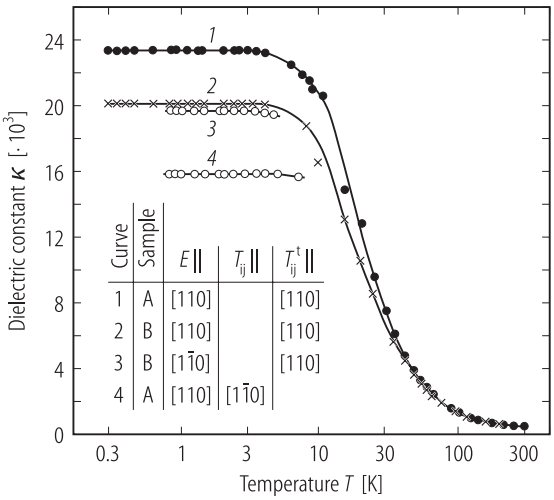

Fig. 1A-8-019. $SrTiO_3$. κ vs. T [79Mul]. Parameter: E, T_{ij}. E: measuring electric field, T_{ij}: externally applied uniaxial stress, T_{ij}^{t}: uniaxial stress introduced by thermal treatment.

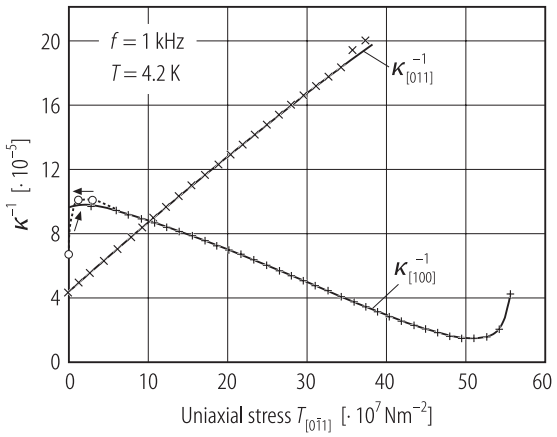

Fig. 1A-8-020. $SrTiO_3$. $\kappa_{[100]}^{-1}$, $\kappa_{[011]}^{-1}$ vs. T 71Bur]. T: Uniaxial stress along $[0\bar{1}1]$. The sample has a single tetragonal domain with its axis along [100]. T = 4.2 K, f = 1 kHz.

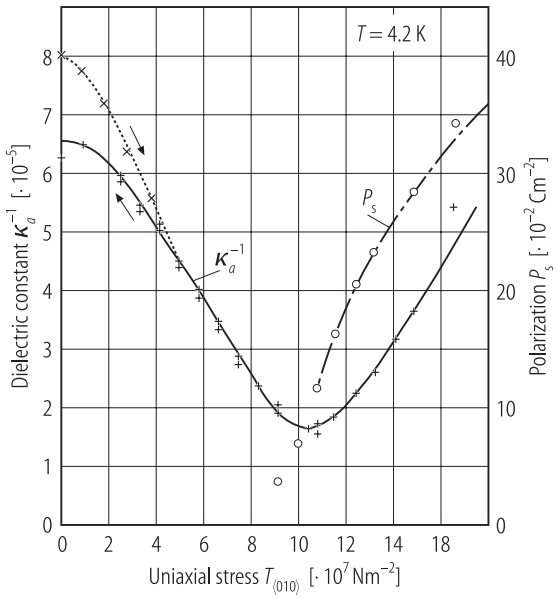

Fig. 1A-8-021. $SrTiO_3$. κ_a^{-1}, P_s vs. $T_{<010>}$ [71Bur]. $T_{<010>}$: Uniaxial stress along <010>. κ at f = 1 kHz, T = 4.2 K.

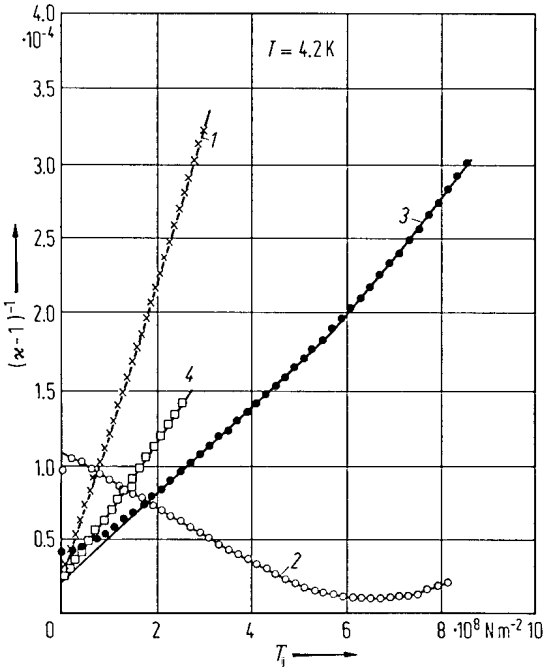

Fig. 1A-8-022. $SrTiO_3$. $(\kappa - 1)^{-1}$ vs. T_{ij} [76Uwe]. T_{ij}: uniaxial stress, E_{ac}: ac field for measuring κ. f = 1...100 kHz.

Curve	T_{ij}	E_{ac}
1	⊥ (010)	∥ [010]
2	⊥ (110)	∥ [001]
3	⊥ (110)	∥ $[1\bar{1}0]$
4	⊥ (110)	∥ [110]

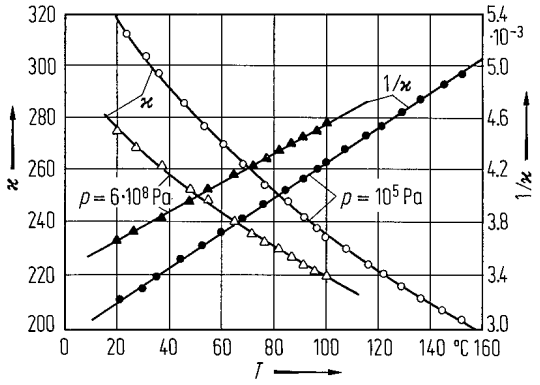

Fig. 1A-8-023. $SrTiO_3$. κ, κ^{-1} vs. T [66Sam]. Parameter: p. f = 1 kHz.

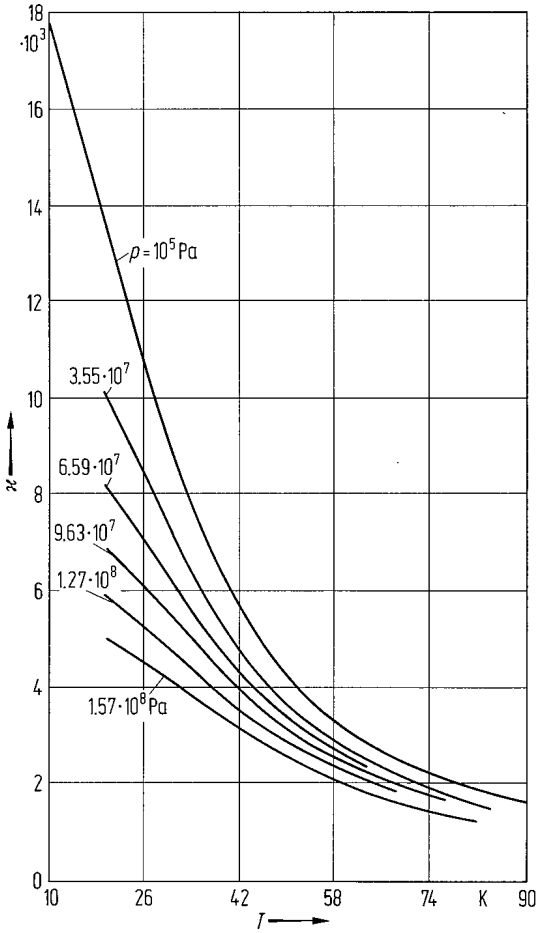

Fig. 1A-8-024. $SrTiO_3$. κ vs. T [67Heg]. Parameter: p. f = 1 kHz.

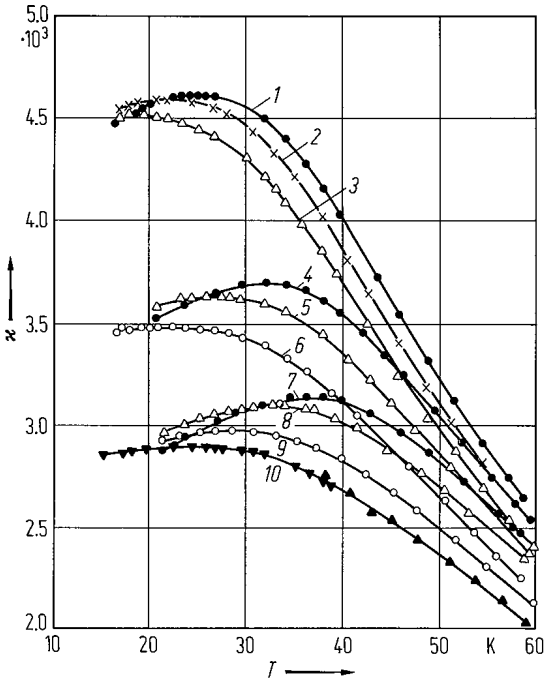

Fig. 1A-8-025. $SrTiO_3$. κ vs. T [74Fre].
Parameter: p, E_{bias}.

Curve	p [$\cdot 10^5$ Pa]	E_{bias} [$\cdot 10^5$ Vm^{-1}]
1	1	3
2	147	3
3	294	3
4	1	4.5
5	294	4.5
6	589	4.5
7	1	6
8	294	6
9	589	6
10	883	6

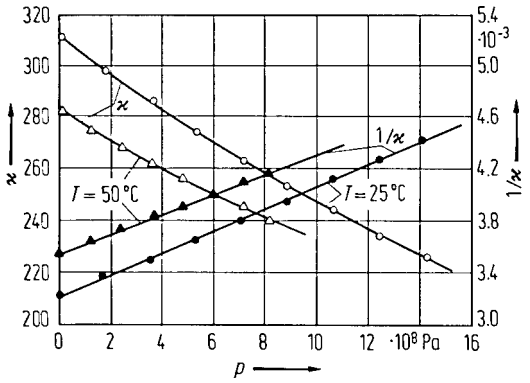

Fig. 1A-8-026. $SrTiO_3$. κ, κ^{-1} vs. p [66Sam]. Parameter: T. f = 1 kHz.

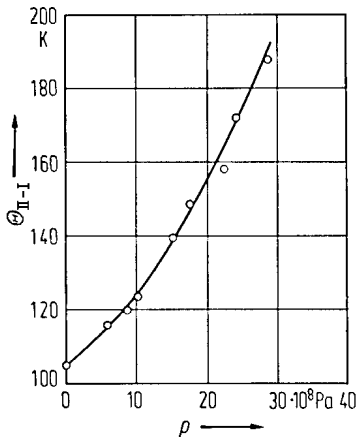

Fig. 1A-8-027. $SrTiO_3$. Θ_{II-I} vs. p [75Oka].

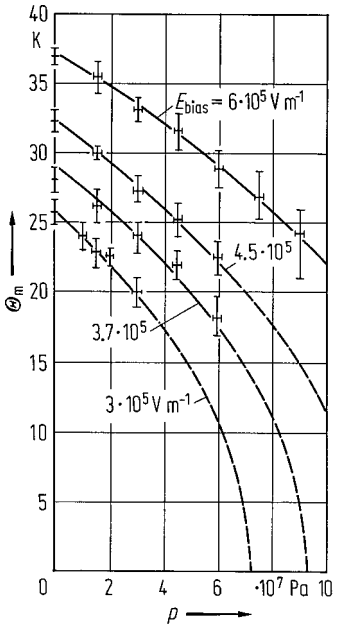

Fig. 1A-8-028. $SrTiO_3$. Θ_m vs. p [74Fre]. Parameter: E_{bias}.
Θ_m: temperature of κ maximum.

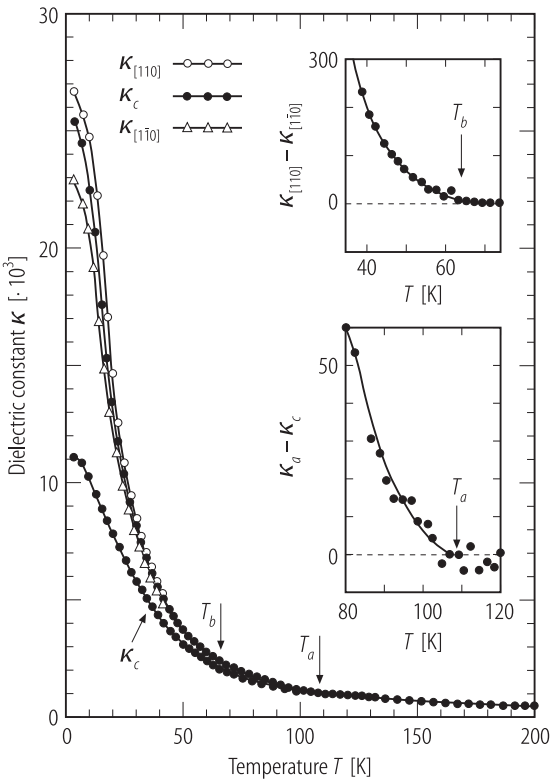

Fig. 1A-8-029. $SrTiO_3$. κ vs. T [71Sak]. Inserts show the details of dielectric anisotropy near T_a and T_b, respectively. f = 10 kHz.

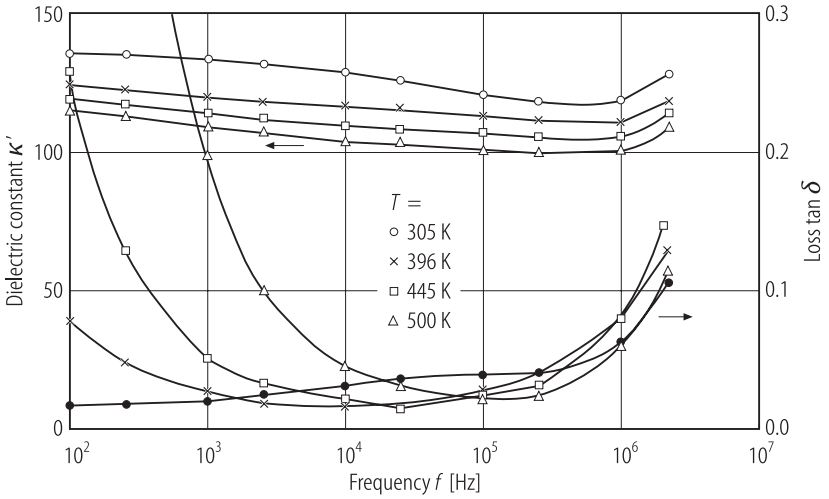

Fig. 1A-8-030. $SrTiO_3$ (thin film). κ', $\tan\delta$ vs. f [93Kam]. Parameter: T. Film thickness: 1.4 μm.

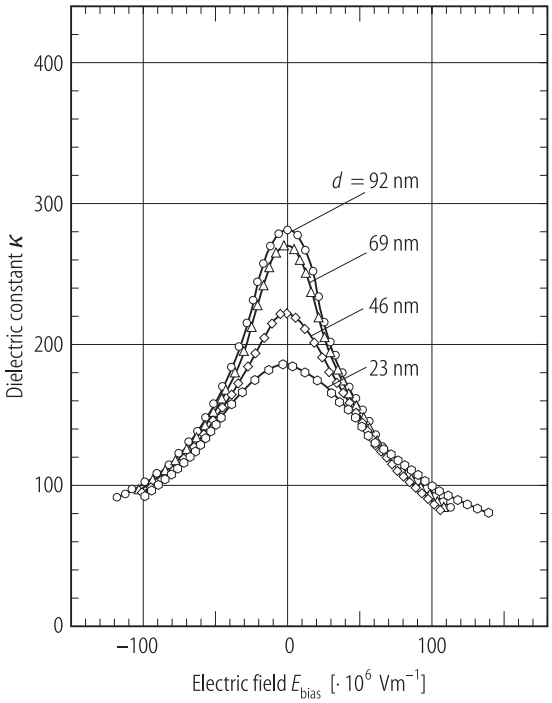

Fig. 1A-8-031. $SrTiO_3$ (thin film). κ vs. E_{bias} [93Abe]. Parameter: *d*, film thickness. f = 100 kHz.

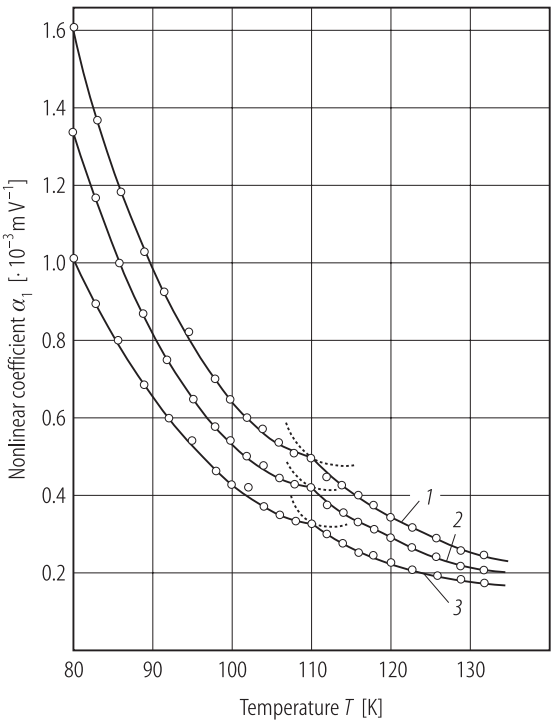

Fig. 1A-8-032. $SrTiO_3$. α_1 vs. T [72Buz]. α_1: first dielectric nonlinear coefficient, $\alpha_1 = (1 / \kappa)\ (\partial\kappa / \partial E)$, where E is measuring ac electric field. Curve *1*: E, $E_{bias} \parallel [100]$, *2*: E, $E_{bias} \parallel [110]$, *3*: E, $E_{bias} \parallel [111]$. $E_{bias} = 7.5 \cdot 10^5$ V m^{-1}.

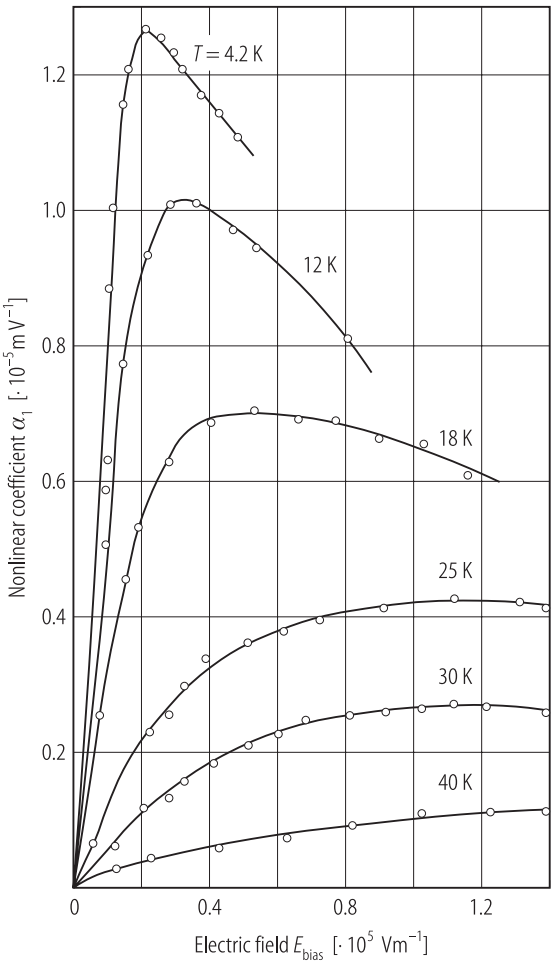

Fig. 1A-8-033. $SrTiO_3$. α_1 vs. E_{bias} [78Iva]. Parameter: T. α_1: first dielectric nonlinear coefficient, $\alpha_1 = (1 / \kappa) (\partial\kappa / \partial E)$, where E is measuring ac electric field. f = 500 MHz.

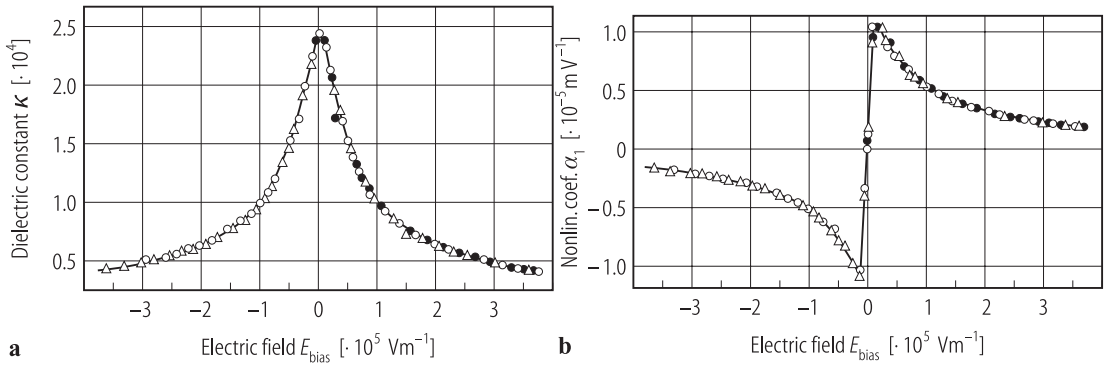

Fig. 1A-8-034. $SrTiO_3$. κ, α_1 vs. E_{bias} [81Bel]. α_1: first dielectric nonlinear coefficient, $\alpha_1 = (1 / \kappa)\ (\partial\kappa / \partial E)$, where E is measuring ac electric field. E, $E_{bias} \parallel [100]$. T = 4.2 K, f = 500 MHz.

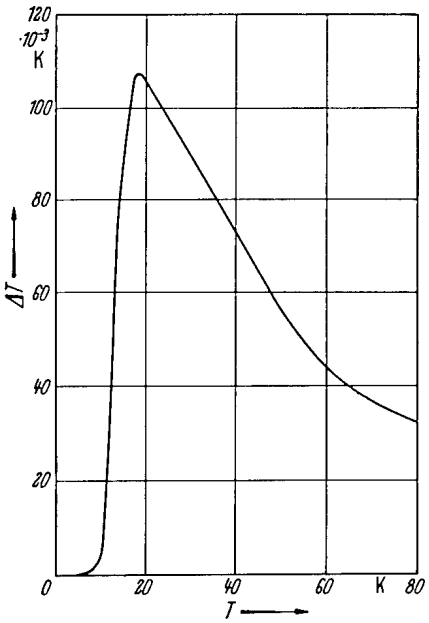

Fig. 1A-8-035. $SrTiO_3$. ΔT vs. T [65Heg]. ΔT: electrocaloric temperature change induced by $E_{bias} = 10 \cdot 10^5$ Vm^{-1}.

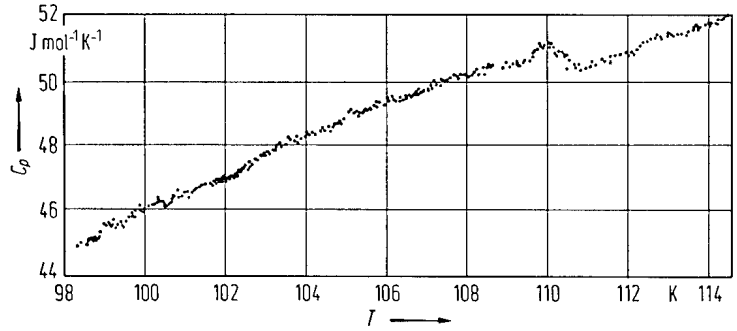

Fig. 1A-8-036. $SrTiO_3$. C_p vs. T [74Fra]. C_p: molar heat capacity at constant pressure.

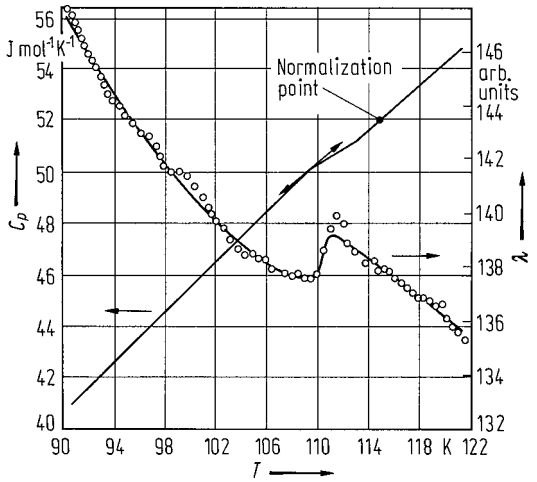

Fig. 1A-8-037. $SrTiO_3$. C_p, λ vs. T [74Sal]. C_p: molar heat capacity at constant pressure, λ: thermal conductivity.

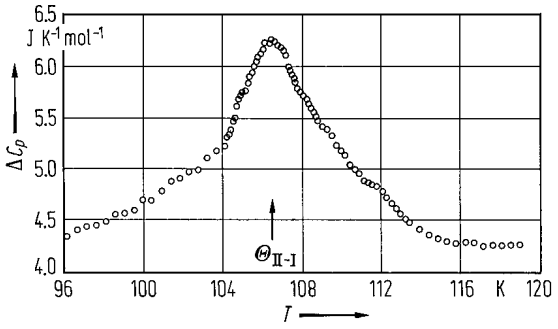

Fig. 1A-8-038. $SrTiO_3$. ΔC_p vs. T [77Hat]. ΔC_p: anomalous part of molar heat capacity at constant pressure. Background part is assumed as $0.432T - 2.809\ \mathrm{J\,mol^{-1}K^{-1}}$.

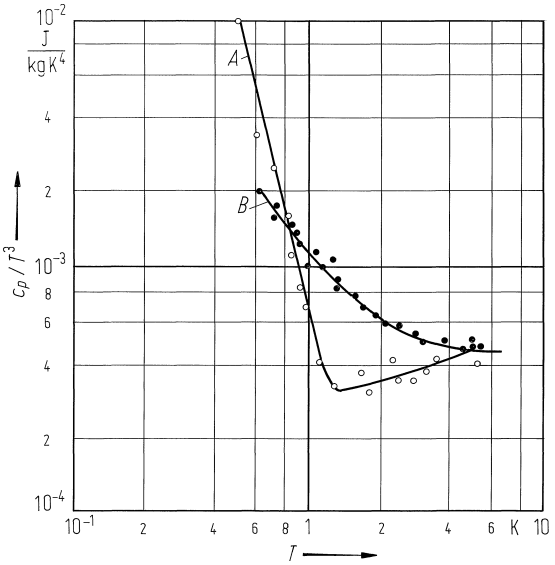

Fig. 1A-8-039. $SrTiO_3$. c_p / T^3 vs. T [84Hen]. c_p: specific heat capacity at constant pressure. *A*: single crystal, *B*: ceramics.

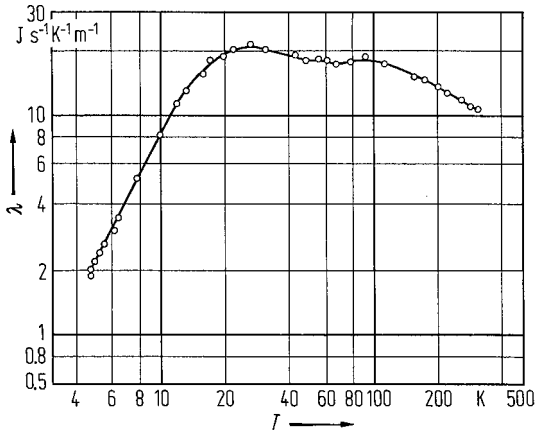

Fig. 1A-8-040. $SrTiO_3$. λ vs. T [65Sue]. λ: thermal conductivity.

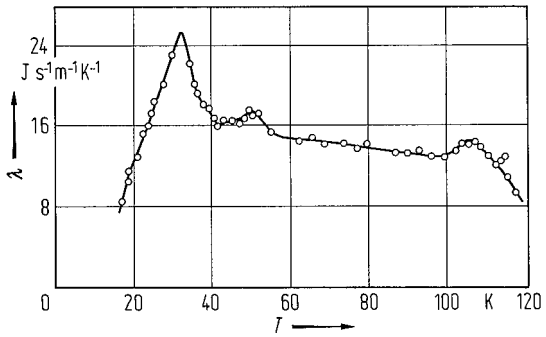

Fig. 1A-8-041. $SrTiO_3$. λ vs. T [66Heg]. λ: thermal conductivity.

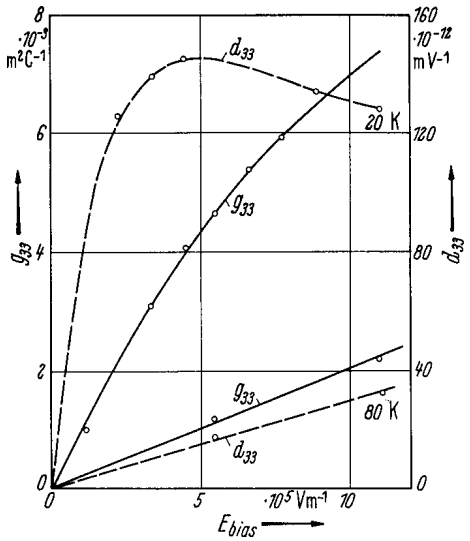

Fig. 1A-8-042. $SrTiO_3$. d_{33}, g_{33} vs. E_{bias} [63Sch]. d_{33}, g_{33}: piezoelectric constant induced by biasing field along [001]. Quasistatic method.

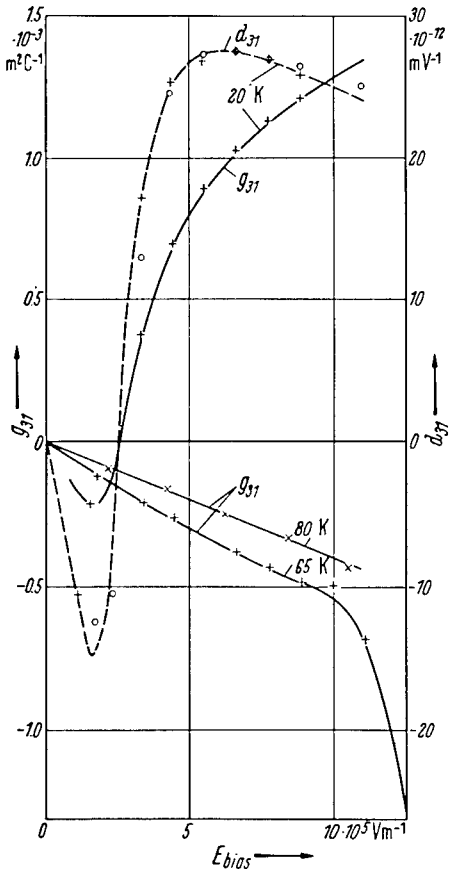

Fig. 1A-8-043. $SrTiO_3$. d_{31}, g_{31} vs. E_{bias} [63Sch]. d_{31}, g_{31}: piezoelectric constant induced by biasing field along [001]. Quasistatic method.

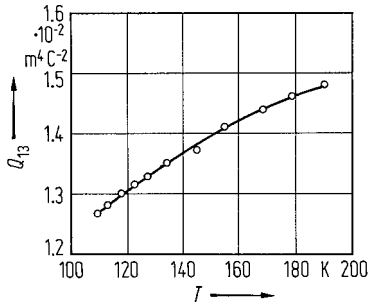

Fig. 1A-8-044. $SrTiO_3$. Q_{13} vs. T [74Sor]. Q_{13}: electrostrictive constant determined by $Q_{13} = d_{31} / (2\ \varepsilon_{33}^{2}\ E_{bias})$ from piezoelectric measurement of d_{31} under E_{bias}.

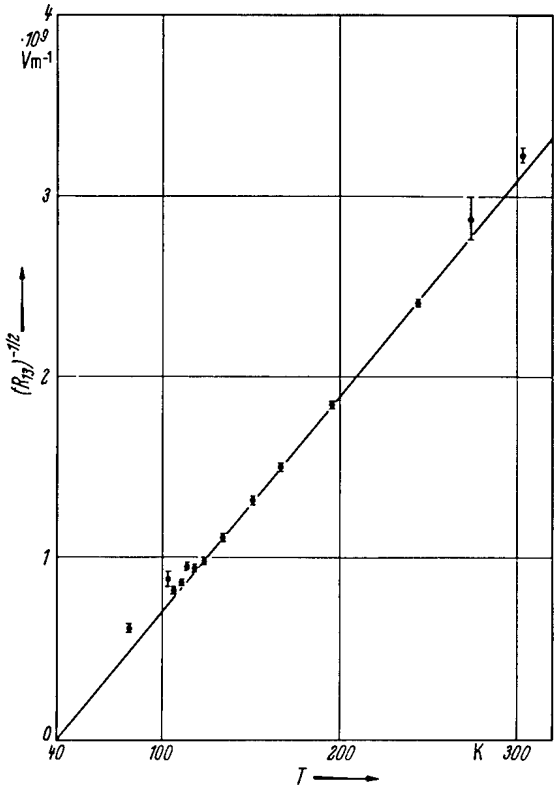

Fig. 1A-8-045. $SrTiO_3$. $(R_{13})^{-1/2}$ vs. T [67Rup]. R_{13}: electrostrictive constant defined by $S_1 = R_{13} E_3^2$. Full curve is given by $R_{13} = 69.2(7)\cdot 10^{-16} (T - 41.48(1))^{-2}$ m^2V^{-2}.

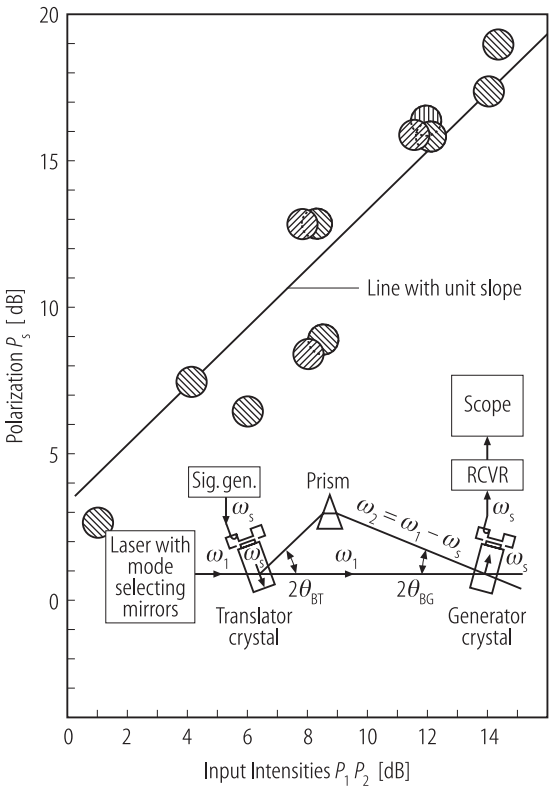

Fig. 1A-8-046. $SrTiO_3$. P_s vs. P_1P_2 [66Cad]. Conversion of light to sound by electrostrictive mixing. P_s: output acoustic power (relative) with frequency ω_s; P_1P_2: product of input optical intensities P_1 (frequency ω_1), P_2 (frequency ω_2). Insert shows experimental arrangement.

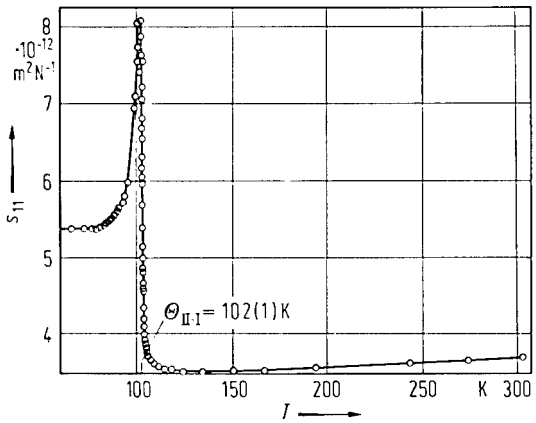

Fig. 1A-8-047. $SrTiO_3$. s_{11} vs. T [67Rup]. Resonance method under $E_{bias} = 15.93 \cdot 10^5$ V m^{-1}.

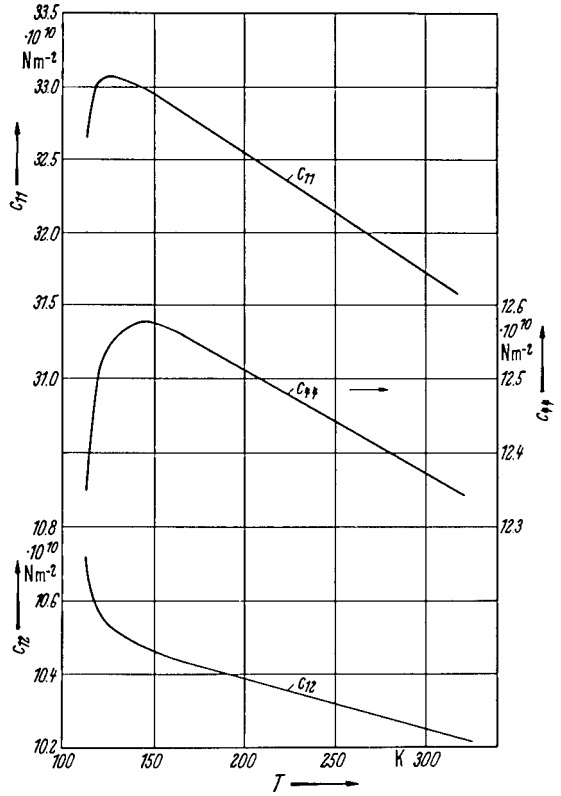

Fig. 1A-8-048. $SrTiO_3$. $c_{\lambda\mu}$ vs. T [63Bel]. Pulse method.

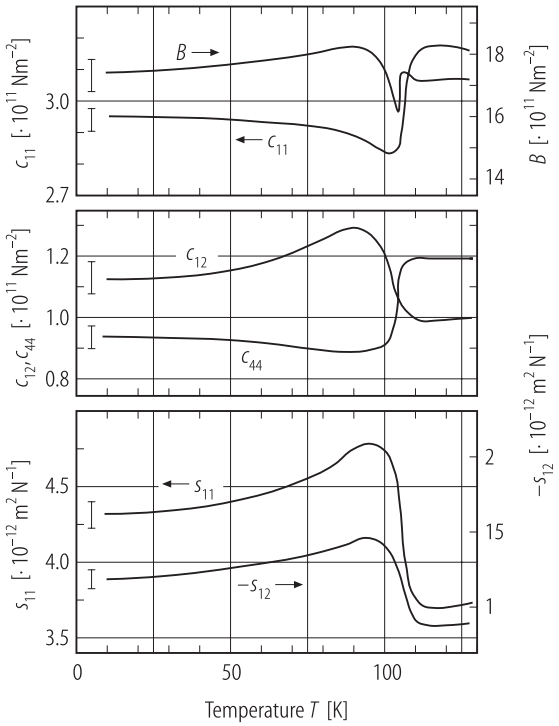

Fig. 1A-8-049. $SrTiO_3$. $c_{\lambda\mu}$, B, $s_{\lambda\mu}$ vs. T [70Reh]. $c_{\lambda\mu}$: elastic constant, B: bulk modulus, $s_{\lambda\mu}$: elastic compliance, in pseudocubic coordinate.

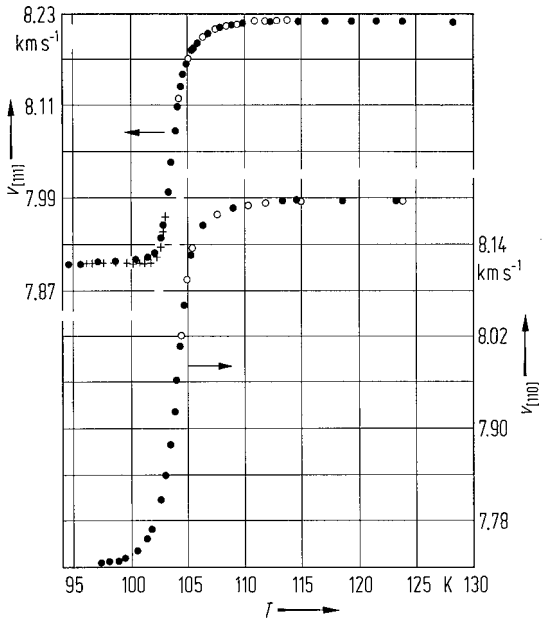

Fig. 1A-8-050. $SrTiO_3$. $v_{[111]}$, $v_{[110]}$ vs. T [70Lut]. $v_{[111]}$ and $v_{[110]}$: velocity of ultrasonic wave propagated along [111] and [110], respectively. Open circles: cooling. Closed circles: warming.

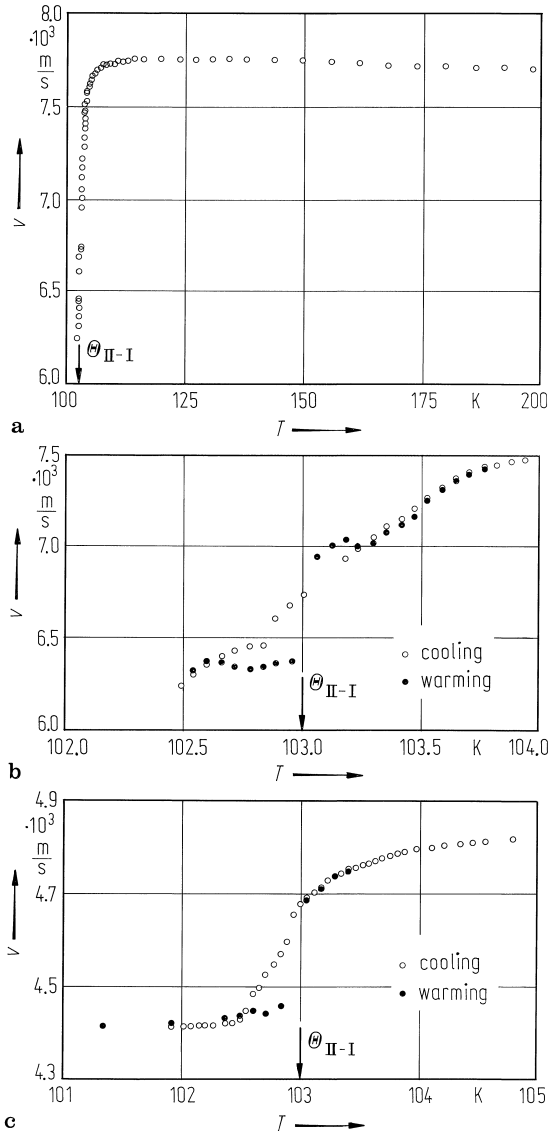

Fig. 1A-8-051. $SrTiO_3$. v vs. T [85Fos1]. v: ultrasonic sound velocity. **(a)** longitudinal sound along a cubic axis, f = 20 MHz; **(b)** close-up view of **fig**ure **(a)** around Θ_{II-I}; **(c)** transverse sound velocity of [100] propagation, f = 17.5 MHz. Specimen was a flux grown crystal.

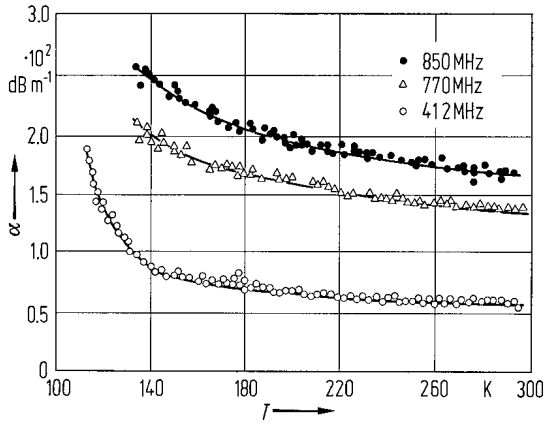

Fig. 1A-8-052. $SrTiO_3$. α vs. T [69Nav]. Parameter: f. α: attenuation coefficient of longitudinal ultrasonic wave propagated along [100].

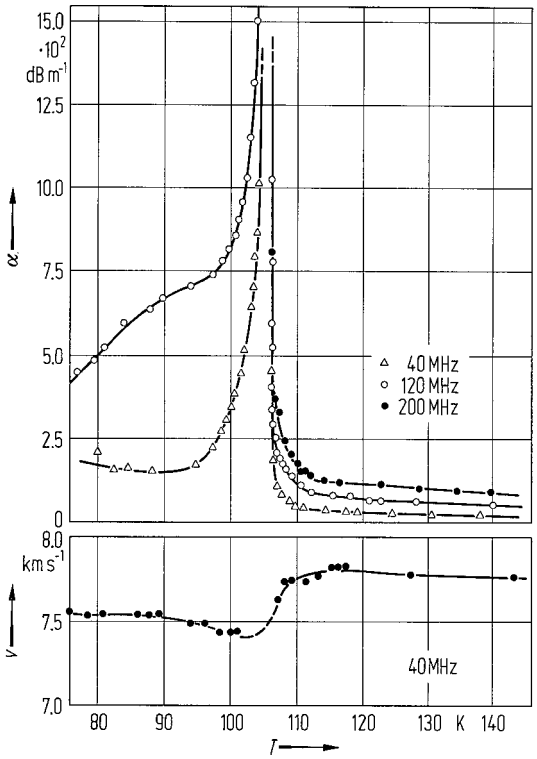

Fig. 1A-8-053. $SrTiO_3$. α, v vs. T [70Reh2]. α and v: attenuation coefficient and velocity of longitudinal ultrasonic wave propagated along [100].

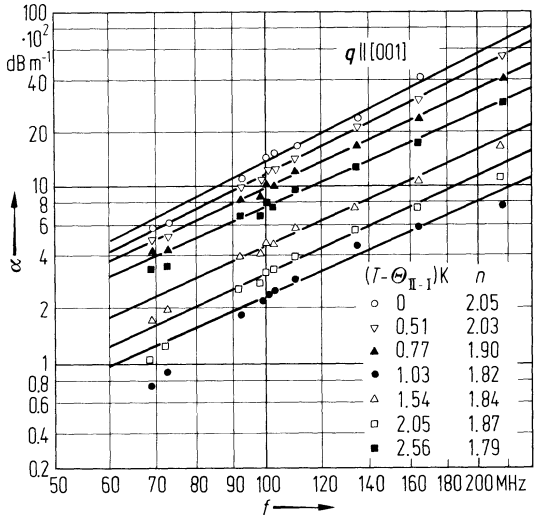

Fig. 1A-8-054. $SrTiO_3$. α vs. f [71Ber]. Parameter: $T-\Theta_{II-I}$. α: attenuation coefficient of longitudinal sound propagated along [100].

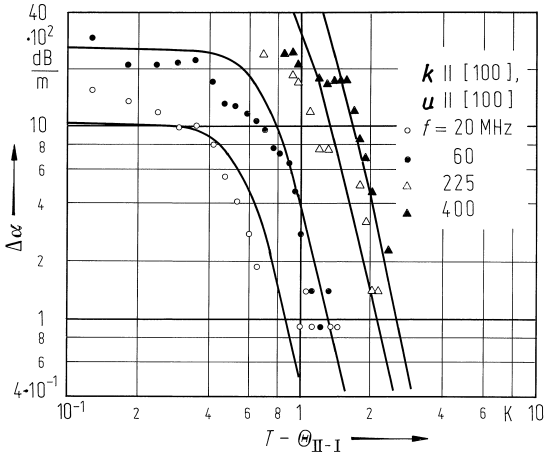

Fig. 1A-8-055. $SrTiO_3$. $\Delta\alpha$ vs. $T-\Theta_{II-I}$ [84Fos1]. Parameter: f. $\Delta\alpha$: anomalous part of absorption for longitudinal sound propagated along [100]. Θ_{II-I} = 103.0 K. $\boldsymbol{u}$: polarization vector of sound wave. Specimen was a flux grown crystal.

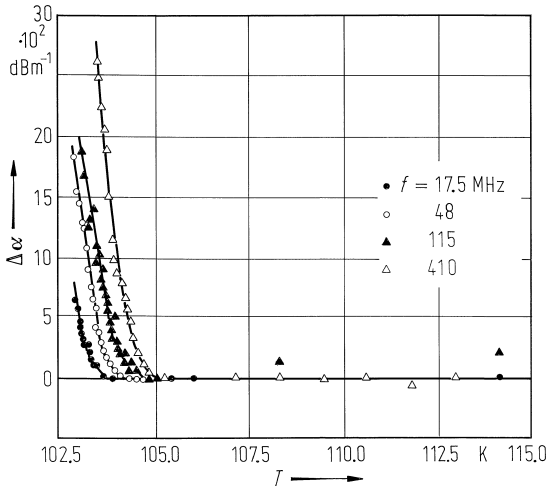

Fig. 1A-8-056. $SrTiO_3$. $\Delta\alpha$ vs. T [85Fos1]. Parameter: f. $\Delta\alpha$: anomalous part of attenuation for transverse sound propagated along [100]. Specimen was a flux grown crystal.

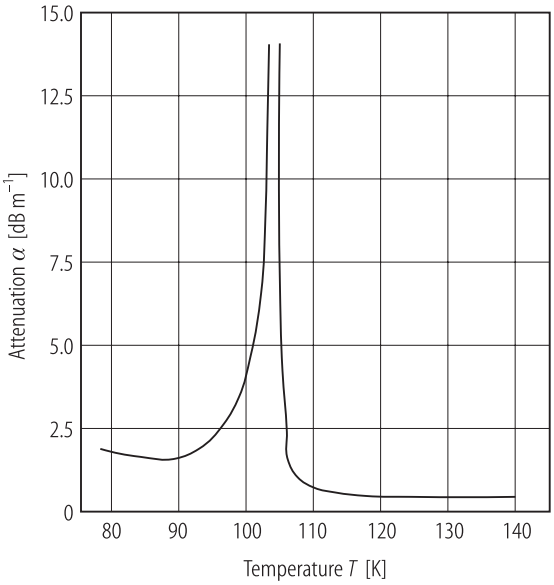

Fig. 1A-8-057. $SrTiO_3$. α vs. T [90Deo]. α: attenuation of longitudinal ultrasonic wave propagated along [100] direction. f = 40 MHz.

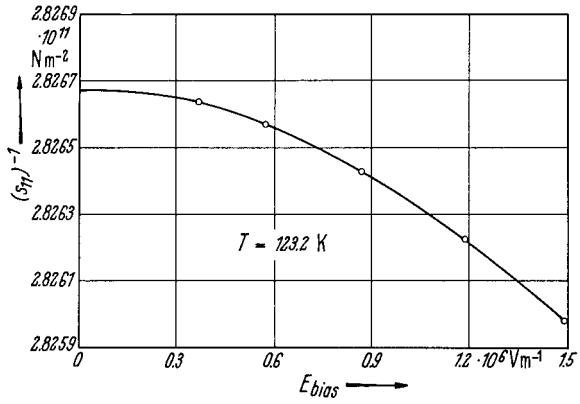

Fig. 1A-8-058. $SrTiO_3$. $(s_{11})^{-1}$ vs. E_{bias} [67Rup]. T = 123.2 K.

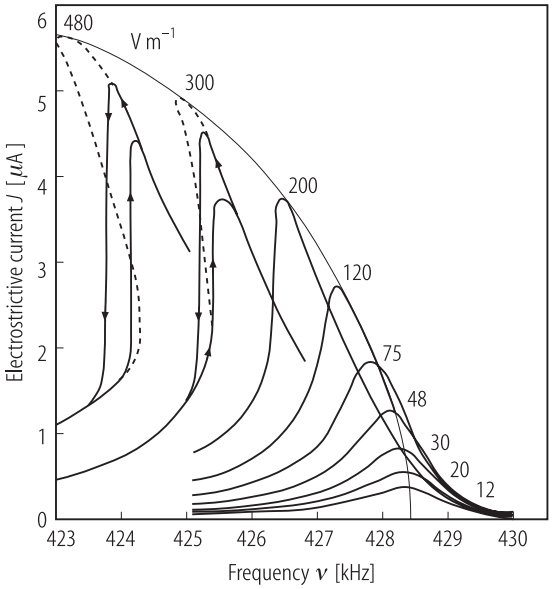

Fig. 1A-8-059. $SrTiO_3$. J vs. ν [73Hoc]. Parameter: E_{driv}. J: electrostrictive current, ν: frequency, E_{driv}: driving field in $V\,m^{-1}$. Solid curve: experimental curve $J(\nu)$; broken curve: projected unstable states; thin curve: locus of horizontal tangent points (represented by a parabola $J^2/\Delta\omega = 7\cdot10^{-5}\ A^2s$).